Mon. Not. R. Astron. Soc. **377,** 1275–1280 (2007) doi:10.1111/j.1365-2966.2007.11684.x

HE 0230–4323: an unusual pulsating hot subdwarf star

C. Koen★

Department of Statistics, University of the Western Cape, Private Bag X17, Bellville, 7535 Cape, South Africa

Accepted 2007 February 28. Received 2007 February 28; in original form 2006 December 21

ABSTRACT

HE 0230−4323 is a known binary, consisting of a subdwarf star and a companion which is not observable in the optical. Photometric measurements reported in this paper have shown it to be both a reflection-effect and a pulsating variable. The dominant pulsation frequencies changed over the course of several nights of observing, from ∼32–39 d^{-1} to ∼8–16 d^{-1}. Observations were obtained through *B* and *V* filters, and the variations in the two wavebands appear to be approximately 180° out of phase.

Key words: binaries: close – stars: individual: HE 0230−4323 – stars: oscillations – stars: subdwarfs – stars: variables: other.

1 INTRODUCTION

The star HE 0230−4323 was identified as an ultraviolet-excess object by the Hamburg/ESO survey (Wisotzki, Reimers & Wamsteker 1991). It was independently classified as a hot subdwarf (sdB) star by Altmann, Edelmann & de Boer (2004) and Lisker et al. (2005). Optical photometry ($V = 13.78$, $B - V = -0.22$, $V - R = -0.11$) was obtained by Altmann et al. (2004), and near-infrared photometry [$J = 13.95$ (0.032), $H = 13.80$ (0.044) and $K_S = 13.86$ (0.068)] is available from the 2MASS catalogue (Skrutskie et al. 2006). Neither the photometry, nor the spectral lines (Lisker et al. 2005), show any sign of the presence of a binary companion. The physical parameters $T_{\rm eff} = 31\,550$ K and $\log g = 5.60$ (Lisker et al. 2005) may therefore be considered reliable.

None the less, despite the lack of direct evidence in the flux distribution, radial velocity variations reveal that star is in fact a close binary with a period of 0.4515(2) d [$f = 2.215(1)$ d^{-1}] – see Edelmann et al. (2005). A lower limit of about 0.2 $M_\odot$ could be set on the unseen companion – as will emerge below, it is most likely a red dwarf star.

This paper is devoted to a description of the results of several photometric observation runs on HE 0230−4323, which led to the discovery that it is a somewhat unusual pulsating variable. The experimental work is described in Section 2, and the analysis of the data in Section 3. Section 4 contains a discussion of the results.

2 THE OBSERVATIONS

All measurements were made with the South African Astronomical Observatory (SAAO) CCD camera mounted on the SAAO 1.0-m telescope at Sutherland, South Africa. The field of view of the camera was 5×5 arcmin^2, which meant that several bright local comparison stars could be measured simultaneously with HE 0230−4323. Prebinning was rapidly abandoned after finding that the results were vastly inferior to those obtained without – however, the penalty was a substantial dead time of close on 60 s while reading out exposures. Observations were obtained alternately through *B* and *V* filters, with I_C replacing *V* for one run. A log of the observations is given in Table 1.

Photometric reductions were performed using an automated version of DOPHOT (Schechter, Mateo & Saha 1993). Differential measurements with respect to two or three of the brightest stars in the field of view were calculated, and the more accurate of the aperture or profile-fitted photometry selected. The known *V* and *B* magnitudes of HE 0230−4323 (Section 1) were used to estimate the brightness of one of the stars in the field of view after the first night's observing; thereafter, these estimated magnitudes were used to set nightly zero-points. The results are plotted in Figs 1 (*B*) and 2 (*V* and I_C).

3 DATA ANALYSIS

A glance at Figs 1 and 2 show (at least) the following.

(i) Large amplitude variability on a time-scale longer than the run length. The amplitude in *V* is slightly larger than that in *B*, while the I_C amplitude is substantially larger than in *B*. Variations in *B* and *V* are more or less in phase on this time-scale.

(ii) Much faster variability is superimposed on the large amplitude changes. The amplitudes in *B* and *V* are comparable.

(iii) The rapid variability appears periodic (see particularly the data from the first and third nights). The occasional apparent disappearance of the fluctuations in a train of cycles suggests multiperiodicity.

(iv) The nature of the rapid variations evolves – the amplitude decreases with time, and the period is much longer during the last night.

(v) A close comparison of the *B* and *V* light curves reveals a substantial phase difference (close to 180°) between the fast variations.

★E-mail: ckoen@uwc.ac.za

Table 1. The observing log: $T_{\rm exp}$ is the exposure time and N is the number of useful measurements obtained during a given run.

Starting time (HJD 2454000+)	Filters	$T_{\rm exp}$ (s)	Run length (h)	N
58.303	*V*, *B*	70, 70	7.0	98, 96
60.297	*V*, *B*	70, 70	5.3	41, 42
61.281	*V*, *B*	70, 70	7.2	102, 99
62.285	*V*, *B*	70, 70	7.0	99, 97
63.287	*I*, *B*	70, 70	7.1	98, 95
67.283	*V*, *B*	70, 90	7.0	97, 88
68.312	*V*, *B*	70, 90	6.3	81, 81

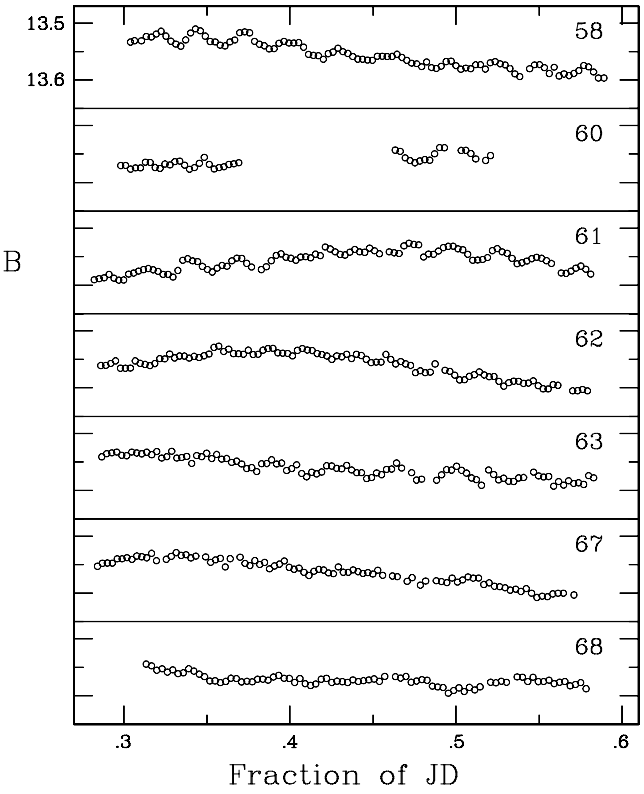

Figure 1. Light curves obtained in the *B* band. The vertical width of each panel is 0.21 mag. Panels are labelled with the last two digits of the Julian Day of observation.

The visual impressions are now investigated quantitatively. The rapid variations are easily extracted by prewhitening the individual light curves by third-order polynomials. The results are in Fig. 3, which compares the higher-frequency *B*- and *V*/*I*-band variations. Remarkably, the blue and yellow/red light variations generally appear to be about 180° out of phase. This holds both for the very rapid changes (JD 2454058, JD 2454061) and for the slower variations (JD 2454068).

Amplitude spectra of the Fig. 3 light curves, excluding the sparse data obtained on JD 2454060, are plotted in Figs 4 and 5. Fairly persistent features occur at low ($\sim$6 d^{-1}), intermediate ($\sim$32–39 d^{-1}) and high ($\sim$59 d^{-1}) frequencies; the corresponding periods are $\sim$4 h, $\sim$45–37 min and 24 min. As is evident from Figs 1 and 2, variability during the last two nights is confined to lower frequencies; these lie in the range 6–16 d^{-1} (periods in the range 4–1.5 h).

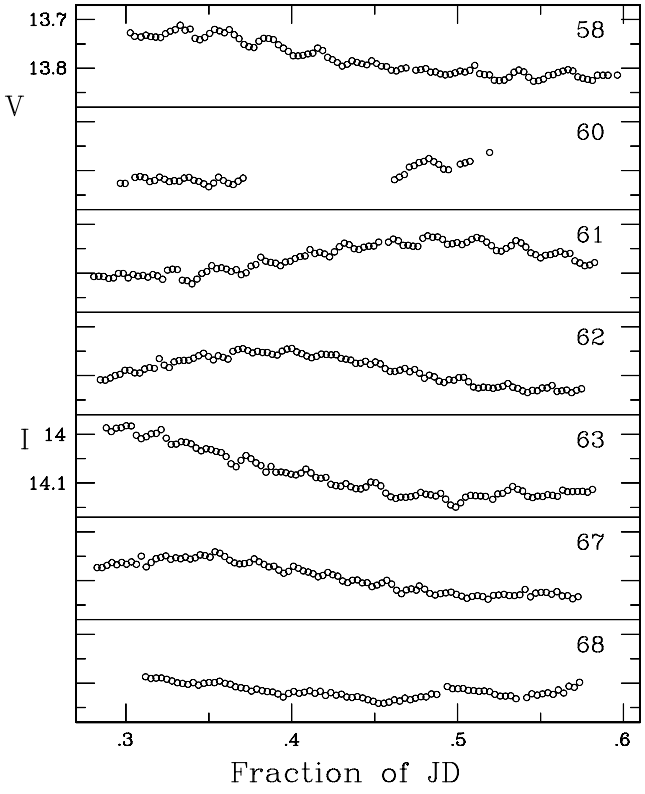

Figure 2. Light curves obtained in the *V* band (panels 1–4, 6–7) and $I_{\rm C}$ band (fifth panel). The vertical width of each panel is 0.21 mag. Panels are labelled with the last two digits of the Julian Day of observation.

Given that the faint companion star is not directly visible in the optical, and that the time-scales are roughly those expected for pulsation in sdB stars, it seems safe to assume that the rapid variability is due to oscillations of the hot star.

The properties of the major frequency components are summarized in Table 2. The agreement between the frequencies of the peaks in the *B* and *V* data is very good. Amplitudes in the blue are mostly, but not always, larger than those in *V*. There are no counterparts in the $I_{\rm C}$-band spectrum for the strongest sinusoidal variations in the *B* band. None the less, it is noteworthy that there is a weak (amplitude 3.3 mmag) $I_{\rm C}$-band feature at 27.2 d^{-1}, which is close to the most-prominent frequency (26.1 d^{-1}) in the *B* data. Furthermore, the strongest $I_{\rm C}$ component is at 52.3 d^{-1}, which is almost exactly twice the frequency seen in the *B* data. Inspection of Fig. 3 brings to light that the pronounced cyclical variations in *B* in the last half of the run are matched by $I_{\rm C}$-band variations, but that the latter appear non-sinusoidal: this suggests that $f = 52.3$ (in $I_{\rm C}$) is indeed the counterpart of $f = 26.1$ (in *B*).

The overall impression is that the frequency content evolves over time, suggestive of relatively short mode lifetimes (perhaps several hours). In view of this, any attempt to extract frequencies from the combined data from different nights might lead to misleading results: a large number of interfering modes would be required to model all the features in the spectra, *none* of which appears permanent.

No completely satisfactory model could be fitted to the large amplitude slow variations. It was found that the best-fitting period is very close to the binary period mentioned in Section 1, hence it may safely be assumed that the variability is due to a reflection effect. Substantial residual power remains at the first harmonic of the

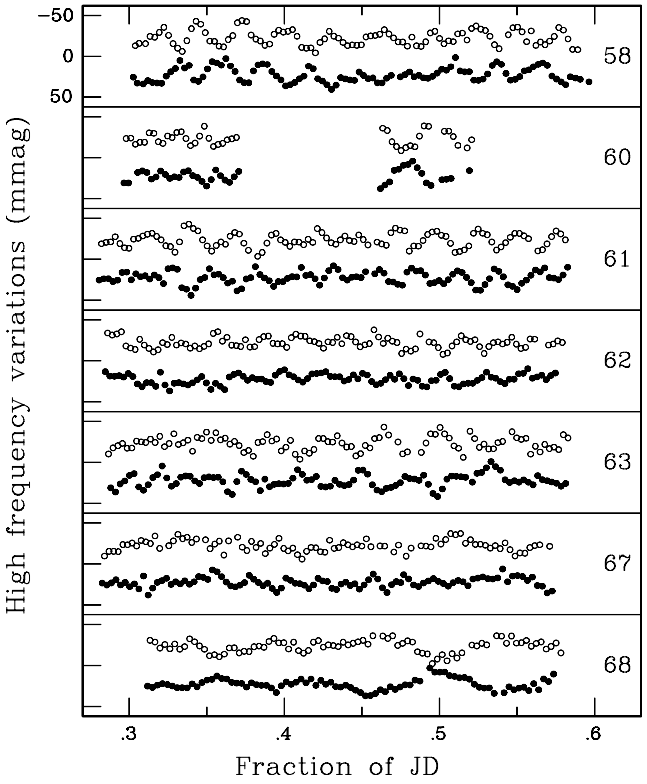

Figure 3. Light curves from Figs 1 (open symbols) and 2 (filled symbols), prewhitened to remove the low frequency variability. Zero-points have been adjusted to offset the two sets of graphs. Panels are labelled with the last two digits of the Julian Day of observation.

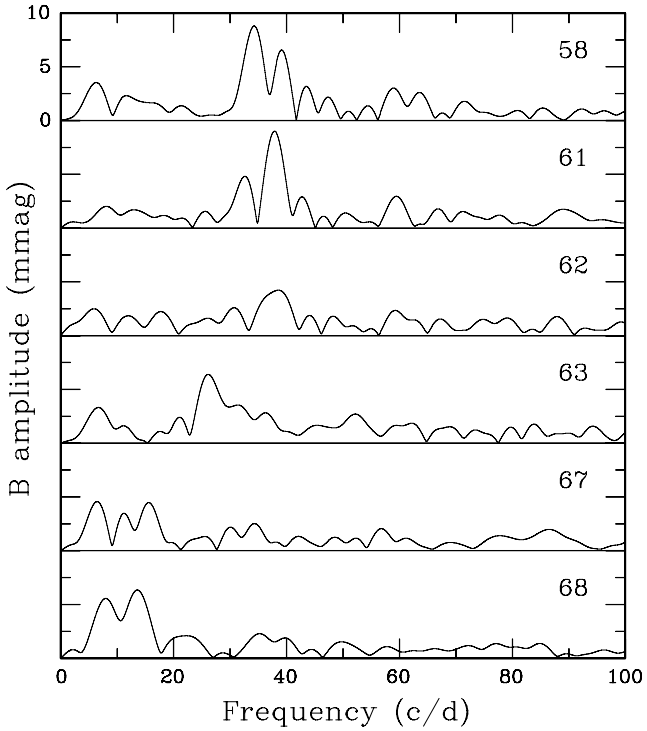

Figure 4. Amplitude spectra of the high-frequency *B*-band data in Fig. 3 (excluding observations from JD 2454060).

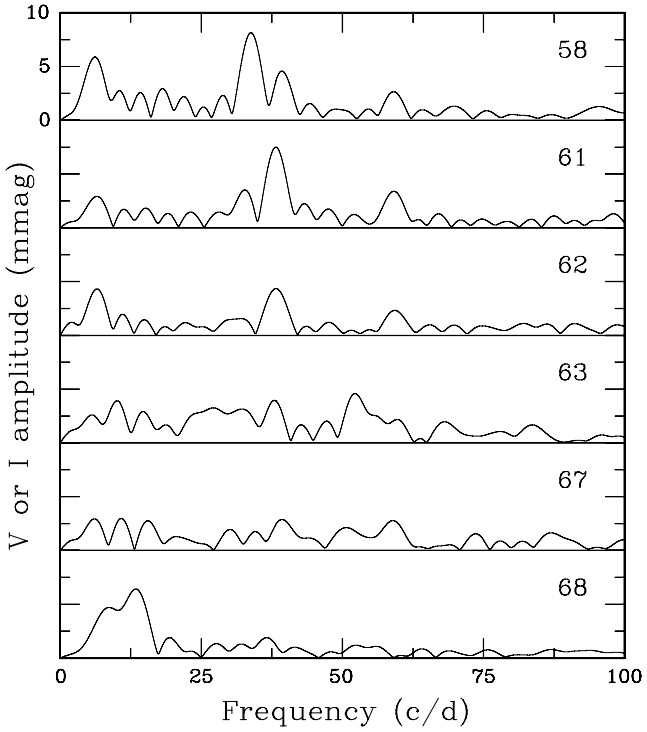

Figure 5. Amplitude spectra of the high-frequency *V* (panels 1, 3–4, 6–7) and I_C (panel 5) data in Fig. 3.

best-fitting frequency, and possibly also at the second harmonic – the ∼6–7 d^{-1} frequency in Table 2. This suggests fitting the truncated Fourier series

$$m_{jk} = \mu_k + \sum_{\ell=1}^{3} A_\ell \cos(\ell f t_{jk} + \phi_\ell) \quad (1)$$

to the data, where m_{jk} is the jth measurement obtained during run k; μ_k is the zero-point for night k; and t_{jk} is the time of the measurement. (Strictly speaking, since the photometry for each night was carefully standardized, the μ_k may be thought redundant. However, in practice there are small apparently random changes in the relative mean brightnesses of the local comparison stars, for reasons which are not obvious.)

The results of fitting the model (1) to the *B* and *V* data are given in Table 3. The *V*-band solution is probably preferred, since the amplitudes are larger and the 95 per cent confidence interval for the frequency narrower. The spectroscopically determined frequency is on the lower boundary of the *B*-band-based confidence interval, but outside the confidence interval derived from the *V*-band data. Fig. 6 shows the data phased with respect to the optimal frequencies.

Since the amplitude of the reflection effect increases with increasing wavelength (and appears to be largest in I_C – see Fig. 2), it may be concluded that the bright spot on the otherwise unseen companion star is relatively cool. This certainly indicates a red dwarf, rather than a white dwarf.

There remains considerable residual power at low frequencies in both data sets, in particular near the first harmonic frequency. The model fit therefore cannot be considered totally satisfactory. A careful examination of the data leads to the suspicion that the low-frequency light curve shape may have changed over the course of the observations, but more extensive observing will probably be

Table 2. A comparison of the most-prominent high-frequency components in the individual *B* and *V* data sets. Amplitudes are given in brackets.

JD 2454050+	Filter	Frequency (amplitude) d^{-1} (mmag)					
58	*B*	6.3 (3.5)			34.3 (8.8)	39.2 (6.6)	59.0 (3.0)
	V	6.2 (5.9)			33.8 (8.2)	39.3 (4.6)	59.1 (2.7)
61	*B*				32.6 (4.8)	37.9 (9.0)	59.5 (3.0)
	V	6.6 (2.9)			32.8 (3.5)	38.3 (7.5)	59.1 (3.4)
62	*B*	5.9 (2.5)				38.6 (4.2)	59.3 (2.4)
	V	6.5 (4.3)				38.3 (4.4)	59.3 (2.3)
63	*B*	6.7 (3.3)		26.1 (6.4)			
	I_C		10.1 (3.9)			38.8 (3.9)	52.3 (4.6)
67	*B*	6.5 (4.6)	11.2 (3.5)	15.6 (4.5)			
	V	6.1 (2.9)	10.9 (3.0)	15.5 (2.8)		39.3 (2.9)	59.0 (2.8)
68	*B*		8.0 (5.6)	13.6 (6.4)			
	V		8.7 (4.7)	13.4 (6.4)			

Table 3. Parameters describing the reflection effect variations. The fourth column gives a formal 95 per cent confidence interval for the frequency, while A_j is the amplitude of the *j*th term in the three-term Fourier series fitted to the reflection light curve.

Filter	Period (d)	Frequency (d^{-1})	95 per cent Confidence (d^{-1})	A_1	A_2 (mmag)	A_3
B	0.450 98	2.2174	(2.2151, 2.2198)	29.4	6.5	2.3
V	0.450 78	2.2184	(2.2171, 2.2198)	40.5	13.8	4.0

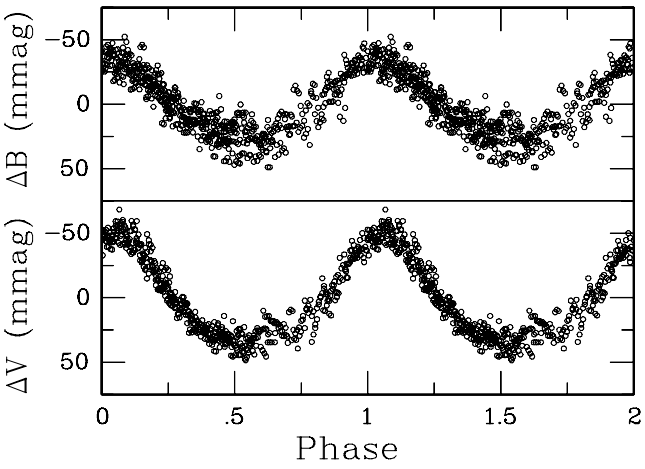

Figure 6. Data folded with respect to the best-fitting binary periods.

required to verify whether such behaviour is in fact in the star's repertoire.

4 DISCUSSION

HE 0230−4323 poses a number of challenges to the current theory of pulsation in sdB stars.

(i) There are two classes of pulsating sdB stars: the rapidly pulsating EC 14026 stars with periods in the range 2–9 min (e.g. Kilkenny 2006), and the slowly pulsating PG 1716 stars with periods typically 1–2 h (e.g. Fontaine et al. 2006). Discounting the 5.9–6.7 d^{-1} entries in Table 2 (which are most likely due to the third harmonic of the binary period), probable pulsation periods of HE 0230−4323 lie in the range 24 min to 3 h, with the most-prominent variations at time-scales of 37–45 min. Thus, although it would probably be classified as a PG 1716 star, HE 0230−4323 is clearly anomalous. Alternatively, it may belong to both pulsator classes – in that case the extraordinarily long p mode periods would need to be explained.

It seems plausible that HE 0230−4323 will be a fairly rapid rotator, given the closeness of its companion and hence the strength of tidal forces in the system. To the best of the author's knowledge the potential influence of rotation on the position of the PG 1716 instability region has not been addressed. In this regard it is noteworthy that in the case of the slowly pulsating main sequence B stars, rotation may shift the instability strip for some modes to higher temperatures (Townsend 2005).

(ii) The region of the $T_{\rm eff}-\log g$ plane inhabited by pulsating sdB stars has been studied observationally by Fontaine et al. (2006). With very few exceptions (five, to be precise) the EC 14026 stars lie in the area $31\,000 < T_{\rm eff} < 37\,000$ K, $5.6 \leqslant \log g \leqslant 5.9$, while all but one PG 1716 stars are cool ($T_{\rm eff} < 30\,000$ K), low-gravity ($\log g < 5.6$) objects. The notion that the temperature boundary between the two classes is near 29 000 K is reinforced by the fact that the two stars known to exhibit both slow and rapid pulsations have temperatures very close to this value.

With $\log g = 5.6$, HE 0230−4323 is on the gravity boundary between the two classes of stars, but its temperature of 31 500 K is substantially higher than that of any PG 1716 star, and within the range of the EC 14026 stars.

(iii) The oscillation modes in the EC 14026 stars are thought to be pressure driven (p modes), while the restoring force of the pulsations in the PG 1716 stars is accepted to be gravity (g modes). While pulsation theory has been successful in producing unstable p modes at gravities and temperatures of the EC 14026 stars (e.g. Charpinet et al. 2006), the same cannot be

said for the g modes in the PG 1716 stars. In particular, modelling predicts that only at higher temperatures ($T_{\rm eff} > 27\,000$ K) will only high-degree ($\ell > 7$) modes be unstable (e.g. Randall et al. 2006). Since such modes ought to be un-observable photometrically (due to the cancellation of many bright and dark areas on the stellar disc), the presence of pulsation in the hotter PG 1716 stars is currently unexplained. If the temperature determination of HE 0230−4323 is accurate, and it is indeed a g-mode pulsator, then perhaps even greater demands are made on the theory.

(iv) The strangest property exhibited by the pulsations in HE 0230−4323 is the approximately 180° phase difference between the high-frequency variations in *B* and *V*. It is particularly remarkable that the phase difference seems very similar for variability on a range of time-scales – compare, for example, the top and bottom panels of Fig. 3.

In order to quantify the comparison between phases in *B* and *V*, sinusoids corresponding to all prominent features in Figs 4 and 5 were fitted to the data in Fig. 3. For each data set, all sinusoids were fitted simultaneously by a non-linear least-squares technique. The results are in Table 4, which also shows the amplitudes and amplitude ratios for the frequencies of interest. The visual impression of large phase differences is confirmed – also the fact that these are often close to 180° (π rad).

It is difficult to think of any explanation for this effect in terms of the binarity of the star, and, furthermore, it does not seem correlated with the binary phase in any way (cf. Figs 1 and 2). This leaves the alternative that it is an intrinsic property of the pulsations.

Two recent theoretical studies dealing with multicolour photometry of pulsating sdB stars are Ramachandran, Jeffery & Townsend (2004, adiabatic models) and Randall et al. (2005, non-adiabatic models). Only the latter set of models provides some insight into possible phase differences between variations seen at different wavelengths: these are predicted to be small, generally less than 10°, but to increase with decreasing period.

According to Randall et al. (2005) the contribution of gravity perturbations to flux variations in the PG 1716 stars is negligible; contributions from temperature perturbations and radius variations dominate. This would suggest that the relative importance of these two factors changes very rapidly with wavelength between 4000 and 5500 Å – which is not predicted by the models.

Both Ramachandran et al. (2004) and Randall et al. (2005) mention that their results apply to non-rotating stars. It is known that rotation can lead to coupling between pulsation modes with different spherical harmonic degree ℓ which have close frequencies – see e.g. Daszyńska-Daszkiewicz et al. (2002) which also contains references to earlier work. Given the dense spectrum of higher radial order g modes expected in the PG 1716 stars, such coupling seems inevitable. One consequence is that the phase differences between variations measured at different wavelengths, may depend very strongly on the angle between the rotation axis and the line of sight.

(v) Ramachandran et al. (2004) and Randall et al. (2005) calculated the relative sizes of amplitudes expected in different wavebands, for various mode degrees ℓ in both EC 14026 and PG 1716 stars. For both types of pulsators, amplitudes decrease with increasing optical wavelength for low-degree ($\leqslant 4$) modes. The data presented in this paper generally seem to conform to this expectation, although there may be some exceptions. An example is the *V* amplitude of the 59.3 d^{-1} variation which is slightly larger then the *B* amplitude on JD 2454061, and the absence of any noteworthy *B*-band power corresponding to high-frequency features in the I_C and *V* bands on JD 2454063 JD 2454067, respectively. However, the data are not of sufficient quality to make very definite statements about the amplitude ratios.

(vi) Kilkenny (2006) (see also Reed et al. 2004) has commented on changes in the frequency content of pulsating sdB star light curves. By some stretch of the imagination it could be argued that a combination of many modes with closely spaced frequencies could have given rise to the examples provided by Kilkenny (2006). The observations of HE 0230−4323 presented here do not seem to afford that luxury – the conclusion that some, or all, modes have lifetimes of only days or hours, seems compelling.

Table 4. The results of fitting sinusoids to the most-prominent features in Fig. 3 by a non-linear least-squares method. Columns 2 and 3 give frequencies, Columns 4 and 5 give amplitudes, Column 6 is the amplitude ratio and Column 7 is the phase difference. The formal standard error is shown in brackets below each value. The variations near 6 d^{-1} were included in the fitting procedure, but results are not shown as these are probably harmonics of the binary light curve.

Date (JD 2454000+)	f_B (d^{-1})	f_V (d^{-1})	A_B (mmag)	A_V (mmag)	A_V/A_B	$\phi_B - \phi_V$ (rad)
58	34.3	33.7	8.0	7.8	0.97	3.2
	(0.20)	(0.15)	(0.71)	(0.62)	(0.12)	(0.26)
	38.9	40.0	4.9	3.7	0.75	−1.6
	(0.33)	(0.32)	(0.72)	(0.62)	(0.17)	(0.47)
	58.7	59.2	2.9	2.6	0.88	4.2
	(0.46)	(0.43)	(0.69)	(0.60)	(0.29)	(0.65)
61	38.1	38.4	9.0	7.7	0.86	4.1
	(0.13)	(0.15)	(0.64)	(0.63)	(0.09)	(0.21)
	31.4	31.5	3.9	3.0	0.75	−2.4
	(0.29)	(0.39)	(0.62)	(0.62)	(0.20)	(0.53)
	59.3	58.7	2.9	3.2	1.10	3.6
	(0.38)	(0.35)	(0.61)	(0.60)	(0.31)	(0.55)
62	38.5	38.2	4.5	4.6	1.02	−2.8
	(0.32)	(0.22)	(0.79)	(0.54)	(0.22)	(0.41)
	59.3	59.6	2.2	2.4	1.06	4.9
	(0.66)	(0.42)	(0.78)	(0.54)	(0.44)	(0.81)
67	15.4	15.6	4.1	2.7	0.65	−2.8
	(0.49)	(0.50)	(0.86)	(0.67)	(0.21)	(0.69)
	11.9	11.0	2.5	2.2	0.87	0.8
	(0.86)	(0.52)	(0.87)	(0.60)	(0.39)	(0.84)
68	13.1	13.4	6.0	6.6	1.11	3.6
	(0.29)	(0.26)	(0.81)	(0.60)	(0.18)	(0.36)
	8.1	9.7	5.1	4.9	0.97	−1.3
	(0.38)	(0.32)	(0.79)	(0.62)	(0.20)	(0.45)

The focus of this paper was the pulsation characteristics of HE 0230−4323, rather than its binary nature. It should be said though that the star is of interest in the latter regard as well. Assuming the companion to the sdB star to be a main sequence star, HE 0230−4323 is only the seventh sdB+M binary to be discovered (cf. Heber et al. 2004). Amongst these it has an unusually long period: aside from PG 1329+159 (Morales-Rueda et al. 2003, $P = 0.25$ d) and HS 2333+3927 (Heber et al. 2004, $P = 0.17$ d), all other systems have orbital periods shorter than 0.12 d (see e.g. the list given by Shimansky et al. 2006).

It seems very likely that the binary configuration of HE 0230−4323 is the result of 'common envelope ejection' evolution (Han et al. 2002; Heber et al. 2004), and that the system is

currently in a pre-cataclysmic variable phase (e.g. Shimansky et al. 2006).

ACKNOWLEDGMENTS

The author is grateful to: those maintaining the SIMBAD database in Strasbourg, France; SAAO for allocating telescope time; and Dr Dave Kilkenny (SAAO) for helpful conversations, and sharing his knowledge of hot subdwarf stars.

REFERENCES

Altmann M., Edelmann H., de Boer K. S., 2004, A&A, 414, 181
Charpinet S. et al., 2006, Balt. Astron., 15, 305
Daszyńska-Daszkiewicz J., Dziembowski W. A., Pamyatnykh A. A., Goupil M.-J., 2002, A&A, 392, 151
Edelmann H., Heber U., Altmann M., Karl C., Lisker T., 2005, A&A, 442, 1023
Fontaine G., Green E. M., Chayer P., Brassard P., Charpinet S., Randall S. K., 2006, Balt. Astron., 15, 211
Han Z., Podsiadlowski Ph., Maxted P. F. L., Marsh T. R., Ivanova N., 2002, MNRAS, 336, 449
Heber U. et al., 2004, A&A, 420, 251
Kilkenny D., 2006, Comm. Asteroseismol., 148, in press
Lisker T., Heber U., Napiwotzki R., Christlieb N., Han Z., Homeier D., Reimers D., 2005, A&A, 430, 223
Morales-Rueda L., Maxted P. F. L., Marsh T. R., North R. C., Heber U., 2003, MNRAS, 338, 752
Ramachandran B., Jeffery C. S., Townsend R. H. D., 2004, A&A, 428, 209
Randall S., Fontaine G., Brassard P., Bergeron P., 2005, ApJS, 161, 456
Randall S. et al., 2006, ApJ, 643, 1198
Reed M. et al., 2004, MNRAS, 348, 1164
Schechter P. L., Mateo M., Saha A., 1993, PASP, 105, 1342
Shimansky V., Sakhibullin N. A., Bikmaev I., Ritter H., Suleimanov V., Borisov N., Galeev A., 2006, A&A, 456, 1069
Skrutskie M. F. et al., 2006, AJ, 131, 1163
Townsend R. H. D., 2005, MNRAS, 360, 465
Wisotzki L., Reimers D., Wamsteker W., 1991, A&A, 247, L17

This paper has been typeset from a TEX/LATEX file prepared by the author.